European Journal of Orthodontics 21 (1999) 633–648

Determination of the centre of resistance in an upper human canine and idealized tooth model

D. Vollmer*,**, C. Bourauel*, K. Maier*** and A. Jäger*
*Poliklinik für Kieferorthopädie and ***Institut für Strahlen- und Kernphysik, Rheinische Friedrich-Wilhelms-Universität, Bonn and **Westfälische Universität, Münster, Germany

SUMMARY The purpose of this investigation was to analyse the influence of geometric and material parameters of a human canine on initial tooth mobility, and the stress and strain profiles in the periodontal ligament. While the material parameters of tooth and bony structures are known within an uncertain limit of approximately a factor of 10, values reported for the elasticity parameters of the periodontal ligament differ significantly. In the course of this study, bilinear behaviour was assumed for the mechanical property of the periodontium.

The finite element model of an elliptical paraboloid was created as an approximation to the geometry of a human canine to reduce calculation time and to determine influences of the geometry on numerical results. The results were compared with those obtained for a realistic human canine model. The root length of both models was 19.5 mm. By calculating pure rotational and pure tipping movements, the centre of resistance (CR) was determined for both models. They were located on the long axis of the tooth approximately 7.2 mm below the alveolar crest for the idealized model and 8.2 mm for the canine model. Thus, the centre of resistance of a human canine seems to be located around two-fifths of the root length from the alveolar margin. Using these results, uncontrolled tipping (1 N of mesializing force and 5 Nmm of derotating momentum), as well as pure translation (additionally about 10 Nmm of uprighting momentum) were calculated. Comparing the idealized and the realistic models, the uncontrolled tipping was described by the parabolic-shaped model within an accuracy limit of 10 per cent as compared with the canine model, whereas the results for bodily movement differed significantly showing that it is very difficult to achieve a pure translation with the realistic canine model.

Introduction

The effect of orthodontic forces on periodontal-tissue remodelling has been the subject of extensive research. The relationship between applied force systems and resulting bone remodelling in terms of tooth movement is not yet fully understood. It is believed that stresses and strains induced in the periodontal ligament (PDL) by the orthodontic force system initiate the bone remodelling process (Gianelly, 1969; Storey, 1973; Davidovitch and Shanfeld, 1975; Davidovitch *et al.*, 1980; Norton *et al.*, 1984; Reitan and Vanarsdall, 1994). Present biomechanical studies indicate that strain, rather than stress is an appropriate mechanical signal initiating orthodontic bone remodelling (Arramon *et al.*, 1994; Middleton *et al.*, 1996; Bourauel *et al.*, 1997, 1999; Turner *et al.*, 1997). The precondition for further understanding of the relationships between stress and strain, on the one hand, and bone remodelling processes on the other is the availability of the mechanical stress–strain distributions within all tissues involved. These stress and strain profiles are determined by the instantaneous mechanical reaction of the tooth in its alveolus upon loading of the crown with an orthodontic force system, i.e. initial tooth mobility. Apart from the elasticity parameters of the tooth (enamel and dentine), the PDL, and

the bone structure (cortical and spongious bone), the influence of the exact geometry of all of these components on the initial tooth mobility is of the utmost importance.

Many different approaches have been undertaken in order to model the reactions of the dento-alveolar complex on the application of a force system. Previous experimental and theoretical research reported in this field indicated the interdependencies between an applied orthodontic force system and the initial tooth mobility, and investigated the distribution of stresses and strains around single- or two-rooted teeth. In earlier photo-elastic studies, the stress distribution around simplified planar tooth models was investigated (Nikolai and Schweiker, 1972; Caputo *et al.*, 1974; Baeten, 1975). The refraction index of transparent media depending on the material stresses in the loaded regions can be determined with optical methods. This stress analysis method is strongly dependent on the materials used and can be applied exclusively to the analysis of extremely simplified models.

Further experimental studies include *in vitro* measurements, performed on enlarged tooth models (Burstone *et al.*, 1978; Pryputniewicz *et al.*, 1978; Pedersen *et al.*, 1990), and on animal and human autopsy material (Dermaut *et al.*, 1986; Fisher *et al.*, 1976; Nägerl *et al.*, 1991; Pedersen *et al.*, 1991), as well as very few *in vivo* measurements (Mühlemann, 1960; Christiansen and Burstone, 1969; Burstone and Pryputniewicz, 1980). The drawbacks of these studies were either a non-sufficient precision in the measurement of the tooth displacements and applied force systems, or just planar registration of the force deflection characteristics.

The theoretical studies which started with planar continuum theoretical investigations (Davidian, 1971; Nikolai and Schweiker, 1972; Nikolai, 1974; Sutcliff and Atherton, 1980) and then transposed into two-dimensional finite element analysis (FEA; Thresher and Saito, 1973; Williams and Edmundson, 1984; Williams *et al.*, 1986) have finally led to fully three-dimensional finite element models (Tanne *et al.*, 1987, 1988, 1991; McGuinness *et al.*, 1991; Cobo *et al.*, 1993). Fundamental relationships could be clarified using analytical mathematical approaches (Synge, 1933; Hay, 1939; Gabel, 1956; Steyn *et al.*, 1978). In general, the first analytical studies were based on planar models, and tried to predict the behaviour of a tooth by setting up and solving a set of differential equations. These equations which describe the interactions of an idealized root with a thin membrane, i.e. the PDL, are rather complex. The real geometries of tooth and tooth supporting structures could only be described approximately, as a large number of idealizations had to be carried out in order to solve the problem.

In FEA, the continous material is subdivided into a large number of finite sections or elements. An accurate model of both anatomy and physical characteristics is required. The loading is applied numerically to the tooth and the resulting tooth movement is calculated. By varying the material parameters of all structures involved, especially those of the PDL which have the smallest Young's modulus, calculated force/deflection diagrams can be adapted to measured ones. Following this procedure, the material parameters can be determined (e.g. Takahashi *et al.*, 1980; Atmaran and Mohammed, 1981; Siegele *et al.*, 1986; Benuzzi *et al.*, 1989; Andersen *et al.*, 1991).

The majority of the theoretical investigations have used standard tooth geometries, and most of the finite element meshes were very coarse. Only one combined study compared experimental and numerical results based on the same specimen (Andersen *et al.*, 1991) to determine linear material parameters of the PDL. A good reference for the material parameters of bone and tooth can be found in Abé *et al.* (1996). An uncertainty of approximately a factor of 10, depending on the assumed density of the bony structures under consideration, can be found in different sources, cited in that review. Thus, the material parameters of bone and tooth are well known. However, a wide range of values of Young's modulus of the PDL can be found in the literature ranging from 0.01 MPa (Tanne *et al.*, 1988) to 100 MPa (McGuinness *et al.*, 1991). These differences can be explained partly by various modelling assumptions, as several authors tried to model hydrodynamic flow processes or damping effects in incompressible media and

others to simulate the behaviour of the ligament under orthodontic loadings.

Especially in the initial phase of tooth displacement, the material non-linearity of the PDL is of importance. Until now, neither the exact non-linear material parameters nor the influence of geometry idealizations on initial tooth mobility have been determined. As material parameters of the ligament and the root geometry have a decisive influence on the stress and strain profiles, and thus influence the orthodontic bone remodelling process, it was the aim of this study to numerically investigate initial tooth mobilities, including material non-linearities and to analyse the effects of geometry idealizations. In a combined experimental and numerical approach, the non-linear elasticity parameters of the PDL and, in subsequent finite element calculations, the possibilities of geometry idealizations were determined. The determination of the elasticity parameters has been described previously (Vollmer *et al.*, 1998) and, thus, only a brief description of this study and the different components used is given below.

Materials and methods

Geometry reconstruction and modelling

A specialized computer program CAGOG (Computer Aided Generator for Orthodontic Geometries; Haase, 1996) was developed to generate most realistic finite element models of a tooth, as well as of the PDL and the bony structures. Specimens are sectioned horizontally every 1.5 mm with an accuracy of 10 mm. Enlarged photographs (magnification: ×10) are taken from the upper side of the cuts which are subsequently digitized. Based on the bitmaps representing the scanned consecutive sections, CAGOG generates a FE mesh semi-automatically (Vollmer *et al.*, 1998). Models consisting of up to 10,000 elements can be generated. Differentiation of the tooth into its components, enamel, and dentine, and of the bone into cortical and spongious bone are possible. The finite element package COSMOS/M (version 1.75a running under Windows NT) and its 8-node isoparametric volume elements were selected to perform the numerical investigations allowing linear, geometrically non-linear and material non-linear calculations.

Using CAGOG a finite element model of an upper human canine was generated from the scanned sections of an extracted tooth. The root length of the tooth was 19.5 mm, with a mesio-distal diameter of 5.7 mm and an oro-vestibular diameter of 7.7 mm at the alveolar crest. As there was no information concerning the thickness of the PDL, an average thickness of 0.2 mm was assumed and automatically generated around the model of the canine's root. Although the thickness of the PDL is not uniform over the root height, this seems to be justified, as the idealized model that will be described in the next section must be generated with a uniform thickness of the PDL as well. The resulting FE model is shown in Figure 1 in a buccal and mesial view. It consists of approximately 3800 elements. Only the shape of the tooth and the desmodontium is shown by the corresponding volume elements. The bony structure is solely indicated by the element nodes. As the calculation refers to initial tooth mobility, the outer geometry of the bony structure does not affect the numerical results (Vollmer *et al.*, 1998). Consequently, this was generated in the shape of a cylinder.

Tooth and root geometry differ significantly from one individual to the other. Thus, it was of interest to determine whether it is possible to find an idealization of the root's geometry, representing the basic dimensions of a tooth without extreme deviations from the real geometry. A suitable approximation to the root of a human canine is an elliptical paraboloid. The length of the canine's root corresponds to the height of the paraboloid, and the long and short axis of the ellipse to the oro-vestibular and the mesio-distal dimensions of the canine at the alveolar crest level. The elliptical paraboloid shown in Figure 1 was generated using the geometrical parameters of the human canine model (Figure 2). It consisted in total of 1500 volume elements. This reduced number of elements, compared with the canine model, results in a significant reduction of calculation time without affecting the stabilty of the results. Additionally, this simple geometry offers the

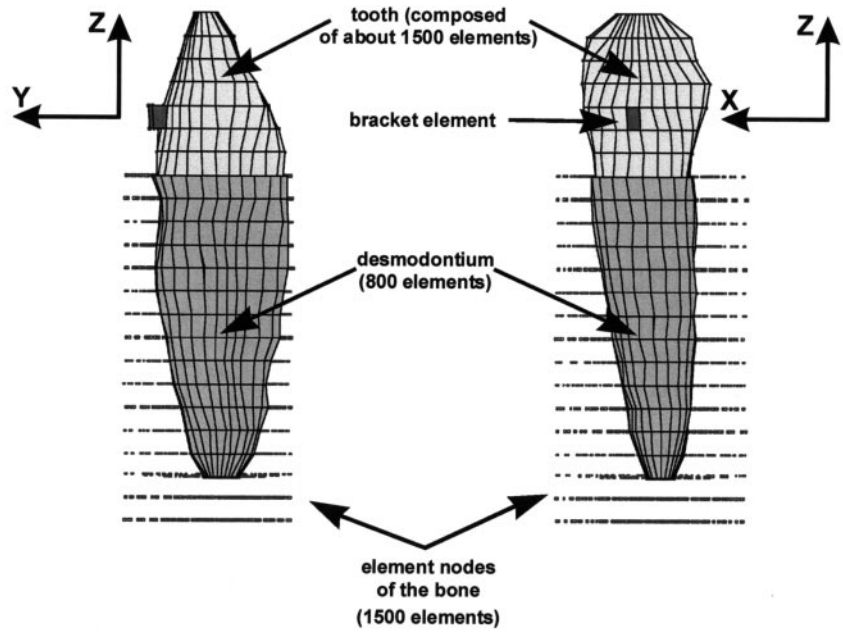

Figure 1 Finite element mesh of an upper human canine in buccal and mesial view. The bony structure is given by the nodal points of the elements to clarify the geometry of the tooth's root and the desmodontium. A steel bracket fixed to the tooth's crown was modelled for the point of force application.

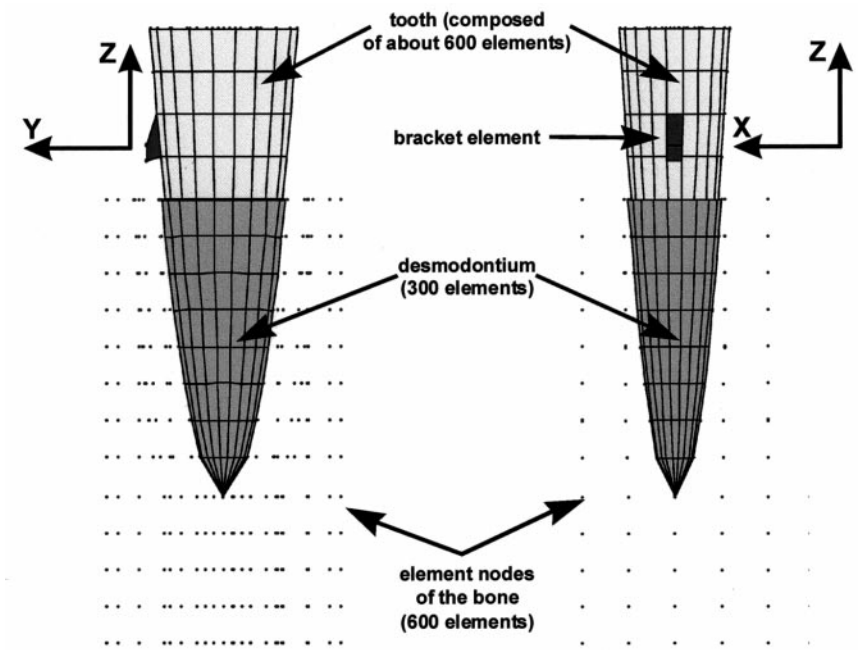

Figure 2 Idealized FE model in the shape of an elliptical paraboloid. The long and short diameters of the ellipse correspond to the oro-vestibular and the mesio-distal diameters of the root in Figure 1. The crown is a straight extension of the root paraboloid at the alveolar crest.

possibility of an automatic generation of the FE mesh based on some analytical relationships. A bracket element made of steel for load application was generated for both the idealized and the realistic model. The centre of the bracket was located at a position of 4.2 mm above the alveolar margin and 5.0 mm buccal with respect to the tooth's long axis.

Material parameters

Material parameters of all structures involved and their influence on the initial tooth mobility have been determined in a preliminary combined experimental and theoretical study (Hinterkausen *et al.*, 1998; Vollmer *et al.*, 1998). A high precision three-dimensional optomechanical set-up (Mobility Measurement System, MOMS) was developed to accurately measure force/deflection characteristics *in vitro*. The measurements have been performed on the segments of swine skulls that were processed in the way described above to generate realistic FE meshes corresponding to the specimen investigated in the MOMS. By performing back calculations and varying the elasticity parameters of the tooth, the bone, and the PDL, the calculated tooth displacements have been fitted to the measured ones and an optimal set of Young's moduli and Poisson's ratios for all structures have been determined.

As a first approximation to the non-linear elastic behaviour of the PDL, a bilinear behaviour of the periodontium was assumed. A low Young's modulus $E_1 = 0.05$ MPa in the first elastic regime and a higher one $E_2 = 0.22$ MPa in the second regime was determined and used in this study (Vollmer *et al.*, 1998). Both linear sections were separated by a certain ultimate strain $\varepsilon_{12} = 7.5$ per cent. A schematic presentation of this elastic behaviour of the PDL is shown in Figure 3. As orthodontics is a long-term phenomenon, it can be assumed that hydrodynamic flow or damping processes play only a minor role. Consequently, the periodontium was assumed as being a compressible medium with a Poisson's ratio of $\mu = 0.3$. The modulus E_1 of the PDL corresponds very well to the elasticity parameters determined by Andersen *et al.* (1991), on the condition that these authors performed their measurements and calculations only in the first elastic regime of the stress/strain curve used to describe the behaviour of the PDL. This underlines the validity of the non-linear material parameters determined on the swine specimens. Further experimentation with human specimens

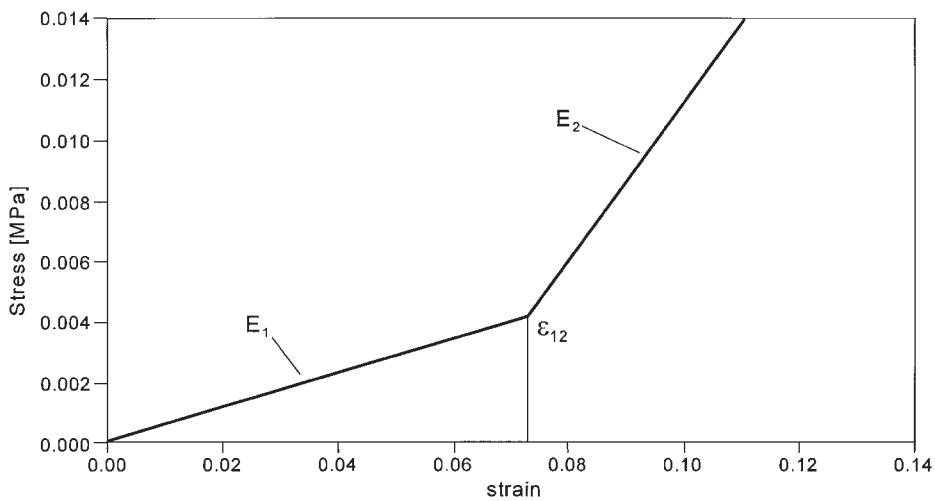

Figure 3 Idealized bilinear behaviour of the periodontium. The lower gradient in the first elastic regime allows a high initial mobility of the tooth for low forces.

Table 1 Mechanical parameters of tooth, desmodontium, and bone used in the study.

Material	Young's modulus (MPa)	Poisson's ratio μ
Tooth	20,000	0.30
Bone	2000	0.30
PDL	Bilinear elastic	0.30
Bracket	210,000	0.30

is being undertaken and the results of the material parameters will be reported in a forthcoming paper.

The elasticity parameters of tooth and bone are at least a factor of 10^4 higher than those of the PDL. Consequently, it is unlikely that a change in the material parameters due to a variation in spongious bone density, or to anisotropic or inhomogenous mechanical behaviour of bone or tooth have a decisive influence on the initial tooth mobility. The parameters used are listed in Table 1. The structures of tooth and bone were modelled as being homogenous and isotropic. The corresponding mean values for a combined elastic behaviour of dentine/enamel and cortical/spongious bone can also be taken from Table 1.

With these material parameters, non-linear finite element calculations were performed with the realistic and the idealized canine model. The resulting movements under various orthodontic loadings were calculated and the CR, as well as stress and strain profiles in the PDL were determined. Force systems used for the calculations and applied to the brackets are listed in Table 2. The co-ordinate conventions were as follows: the *X*-axis was defined by a line connecting the distal to mesial, the *Y*-axis by a line from the oral to buccal and the positive *Z*-axis by a line running from apical to coronal.

Results

Figures 4–7 show the results of the calculations. The initial tooth displacements of the human canine model and the idealized model were compared using the total displacements of the nodal points of the models [i.e. total displacement = $(x^2 + y^2 + z^2)^{1/2}$]. The displacements were enlarged by a factor of 20. In Table 3 the movements are listed in terms of the three translations and three rotations with respect to the centre of the bracket.

Loading both the idealized model and the canine with a rotating momentum of M_Z = 10 Nmm the models showed a nearly pure distal rotation of the bracket around the tooth's long axis (Figure 4). The calculated total displacement was approximately 10 per cent higher for the idealized model than for the realistic canine, both having the centre of rotation (C_{Rot}), i.e. the centre of resistance (CR), on the tooth's long axis. The calculated movement of the bracket was R_Z = 0.810 degrees and R_Z = 0.905 degrees for the canine and the idealized model, respectively (Table 3). The components of translation T_X result from the rotation around the tooth's axis and display the deflection of the bracket due to the rotation. Significant side components (T_{YZ}, R_X) were calculated for the human canine model, whereas the loading of the idealized model resulted in a rotation with only minor side effects.

When loading both models with a pure tipping momentum of M_Y = 10 Nmm, the location of the CR in the sagittal plane could be identified as the C_{Rot} (Figure 5). In both cases the position was below one-third (i.e. 6.5 mm) of the root length

Table 2 Force systems used in the calculations.

Type of tooth movement	Applied force system
Mesial tipping of the crown around the CR	M_Y = 10.0 Nmm
Distal rotation of the bracket around the CR	M_Z = 10.0 Nmm
Uncontrolled mesial tipping	F_X = 1.0 N; M_Z = 5.0 Nmm
Pure translation (bodily movement)	F_X = 1.0 N; $M_Y \approx$ –10.5/–11.1 Nmm; M_Z = 5.0 / 4.4 Nmm

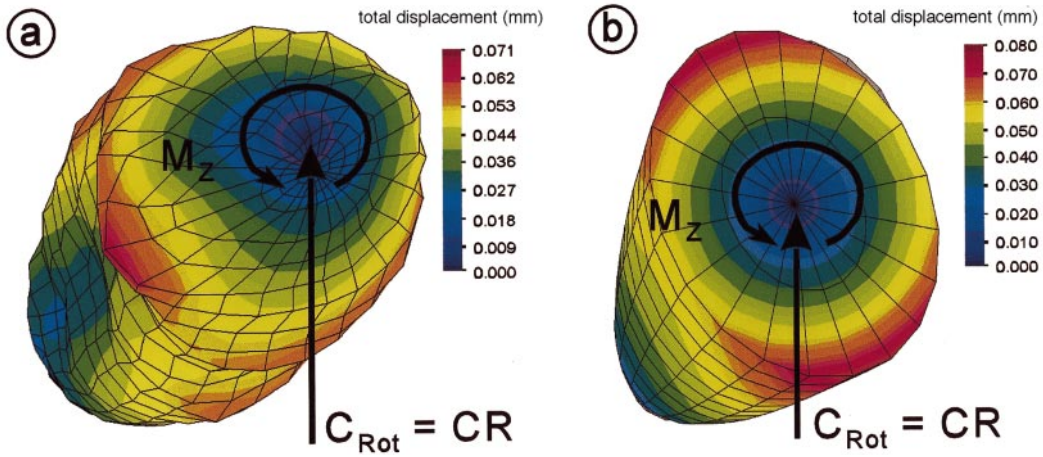

Figure 4 Calculated pure rotation of the human canine model (left) and the idealized model (right) with a pure rotating momentum of M_Z = 10 Nmm. The movement is given in terms of the total displacement of the nodal points. The displacements are enlarged by a factor of 20 and are colour coded with a scaling to the maximum in each case. The minimum of the movement (centre of rotation, dark blue) coincides with the CR. It is located on the tooth's long axis for both models. Due to its smoother surface the idealized model displays about 10 per cent higher rotation.

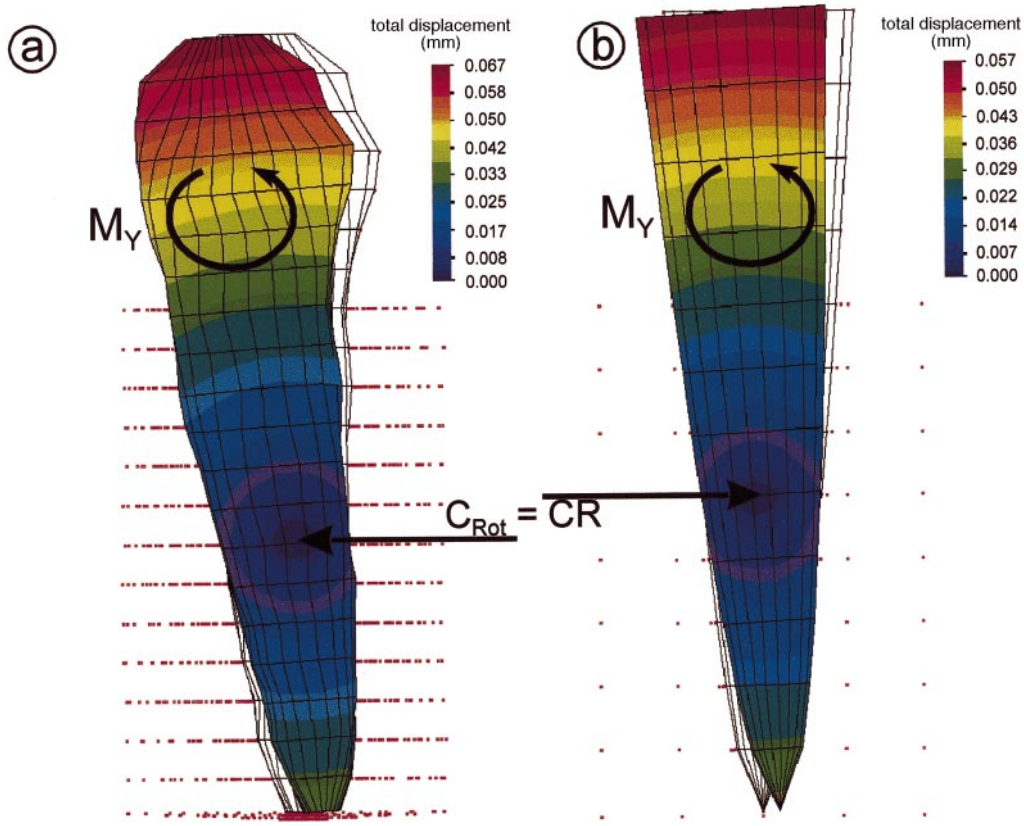

Figure 5 Pure tipping for both models at a tipping momentum of M_Y = 10 Nmm. Again the CR coincides with the minimum of the displacements (dark blue). It is located below a value of one-third of the root length for both models.

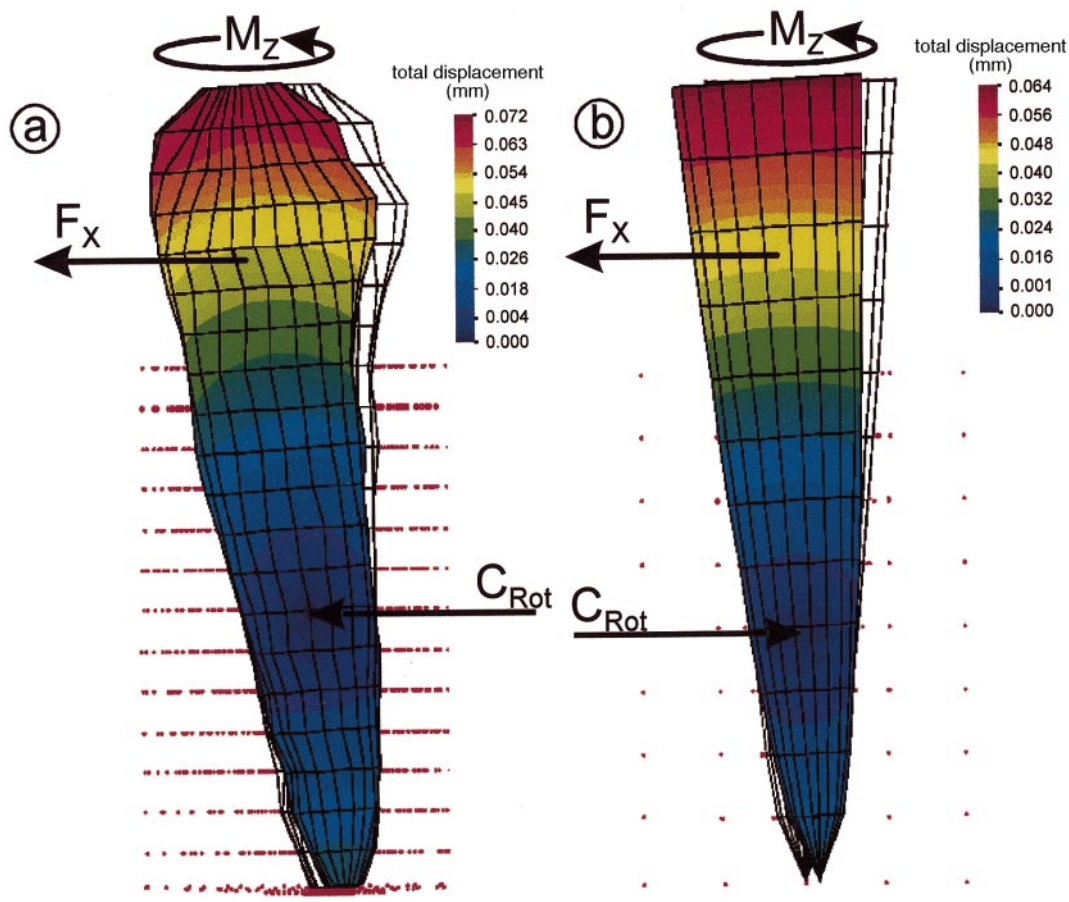

Figure 6 Uncontrolled tipping at a mesializing force of 1 N and a derotating momentum of 5 Nmm. Due to the lower CR the human canine model displays a higher tipping than the idealized model.

7.25 and 8.20 mm underneath the alveolar crest for the idealized and the human canine models, respectively. The total amount of movement was higher for the canine model ($R_Y = 0.199$ degrees) than for the elliptical model ($R_Y = 0.180$ degrees). This indicates a slightly higher stiffness of the complete idealized model consisting of tooth, PDL, and alveolar bone, i.e. the idealized root geometry has a higher resistance towards a movement through the PDL than the realistic one.

Figures 6 and 7 display the calculated displacements of the idealized, and the human canine model after loading with force systems for uncontrolled tipping and bodily tooth movement. Loading the tooth with a force system consisting of a mesializing force and a derotating momentum resulted in an uncontrolled tipping, i.e. the tooth rotated around a C_{Rot} lying in the lower third of the root (Figure 6). The C_{Rot} was located more apically for the human canine model than for the elliptical model and, thus, the amount of tipping R_Y was markedly larger (0.208 and 0.168 degrees, respectively, Table 3). This was due to the fact that the CR of the human canine model lies more apically than for the idealized model and, thus, the resulting tipping momentum from the mesializing force ($F_X = 1$ N) was higher. With a derotating momentum of M_Z = 5 Nmm, a complete compensation of the rotation around the tooth's long axis (R_Z) could be achieved for the idealized model, whereas the human canine model displayed a mesial rotation of the bracket of about –0.072 degrees, although the distance of the point of force application

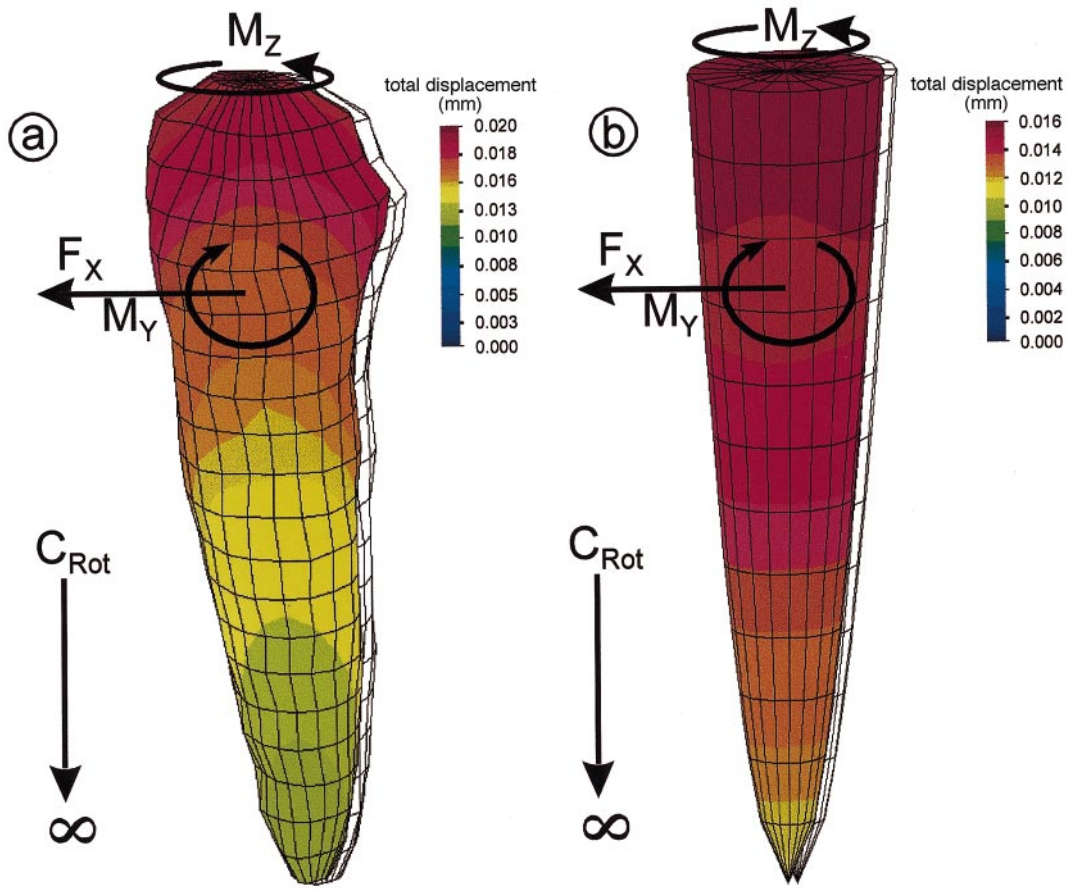

Figure 7 The force system for bodily tooth movement of the canine model had to be varied to achieve a pure translation, whereas the idealized model displayed a nearly perfect bodily tooth movement.

(centre of bracket) to the long axis of the tooth was 5.0 mm.

This can also be seen in the simulations of bodily tooth movement. Applying additionally uprighting moments of M_Y = –10.5 Nmm and M_Y = –11.5 Nmm to the bracket of the idealized and the canine models, respectively, a pure translation should be achieved. A nearly perfect bodily tooth movement could be simulated with this force system for the elliptical paraboloid. However, the results for the canine model showed distinct rotating components with the force system derived from the location of the CR, determined above. A variation of the force system showed best results for an uprighting momentum of M_Y = –11.1 Nmm and a derotating momentum of M_Y = 4.4 Nmm (Tables 2 and 3, and Figure 7), a discrepancy of approximately 10 per cent in the torque values between the force system of pure translation for the idealized and the canine model. A pure translation could not be achieved with a force system directly derived from the position of the CR.

Figure 8 shows the distribution of the strains along the *Z*-axis for those elements of the PDL lying in the mesio-distal direction of both models and determined for the uncontrolled tipping in a mesial direction. The curves run quite similar for the canine (upper part) and the idealized model (lower part) both regarding the absolute values and the gradients. The smooth surface of the idealized root resulted in a very straight curve with the exception of a deviation at the apex, resulting from the special type of mesh generation at the

Table 3 Summary of the calculated initial tooth displacements for the human canine and the idealized model.

	T_X (µm)	T_Y (µm)	T_Z (µm)	R_X (°)	R_Y (°)	R_Z (°)
Rotation around the tooth's axis						
Human canine	–62.6	–8.0	–4.5	0.050	0.002	0.810
Elliptical model	–78.8	–0.6	–1.7	0.000	0.000	0.905
Mesial tipping around the CR						
Human canine	42.8	–0.9	–5.7	0.003	0.199	–0.005
Elliptical model	31.5	0.0	–1.3	0.000	0.180	0.001
Uncontrolled mesial tipping						
Human canine	45.7	1.7	–4.9	0.002	0.208	–0.072
Elliptical model	37.8	0.0	–1.7	0.000	0.168	0.000
Translation						
Human canine	16.1	1.0	–0.8	0.000	0.012	–0.032
Elliptical model	15.8	0.0	–0.4	0.000	0.000	0.001

lower tip of the model (compare Figure 2). The irregular root surface of the canine, however, leads to variations from a straight line of the strain distribution. For both models the normal strain ε_X had the highest (approximately 0.15) and the shear strain around the *Y*-axis the second highest value ($\gamma_{XZ} = 0.05$). Similar maximum values could be determined for loading PDL elements in the oro-vestibular direction (Figure 9). The strain components were interchanged ($\gamma_{XY} = 0.15$ had the highest value, $\gamma_{XZ} = 0.05$ the second highest) and there were no normal strains ε_X, i.e. no normal strains in the direction of movement. Strains in the bone did not exceed $2*10^{-6}$ in each of the cases and thus are a factor of 10^5 smaller than in the PDL.

Figure 10 depicts the stress distribution in the mesio-distal PDL elements over the *Z*-axis for uncontrolled tipping. The stress σ_X corresponds to the strain ε_X, but as a bilinear mechanical behaviour of the PDL is assumed, the course of the curves clearly differ from those of the strain distributions. A value of 7.5 per cent (0.075), for example, is exceeded at a root height of approximately 15 mm and, thus, there is a steep increase in stress at the alveolar crest. Consequently, a pronounced non-linear relationship between the stress components and the root height results from the assumed non-linear behaviour of the PDL with maximal stresses of about $\sigma_X = 0.04$ N/mm^2 at the alveolar crest.

Discussion

It was the aim of this study to determine whether it is possible to find an idealization of a typical root geometry and to derive the most relevant characteristics of a tooth from this idealized root shape by means of FE methods. The human canine was chosen as a model to perform this study. Root shapes differ significantly from one individual to another. The geometry of a canine root can be described by its height and its oro-vestibular, as well as its mesio-distal diameters at the level of alveolar crest. As the root diameter has a roughly parabolic dependency from the root height, several authors used rotational paraboloids as an approximation to the root shape (e.g. Burstone *et al.*, 1978; Pedersen *et al.*, 1990), but as the oro-vestibular and mesio-distal dimensions are different, an elliptical cross-section seems to be a more appropriate approximation to the canine's root.

Initial tooth displacements and, to a certain extent, orthodontic tooth movements can be characterized with the help of the CR. When calculating a pure rotation for the idealized and the human canine model, respectively, the amplitudes of movement are larger for the idealized model than for the canine. This behaviour can be explained by the smoother surface of the idealized model. On the other hand, the type of movement is not influenced by the idealization as

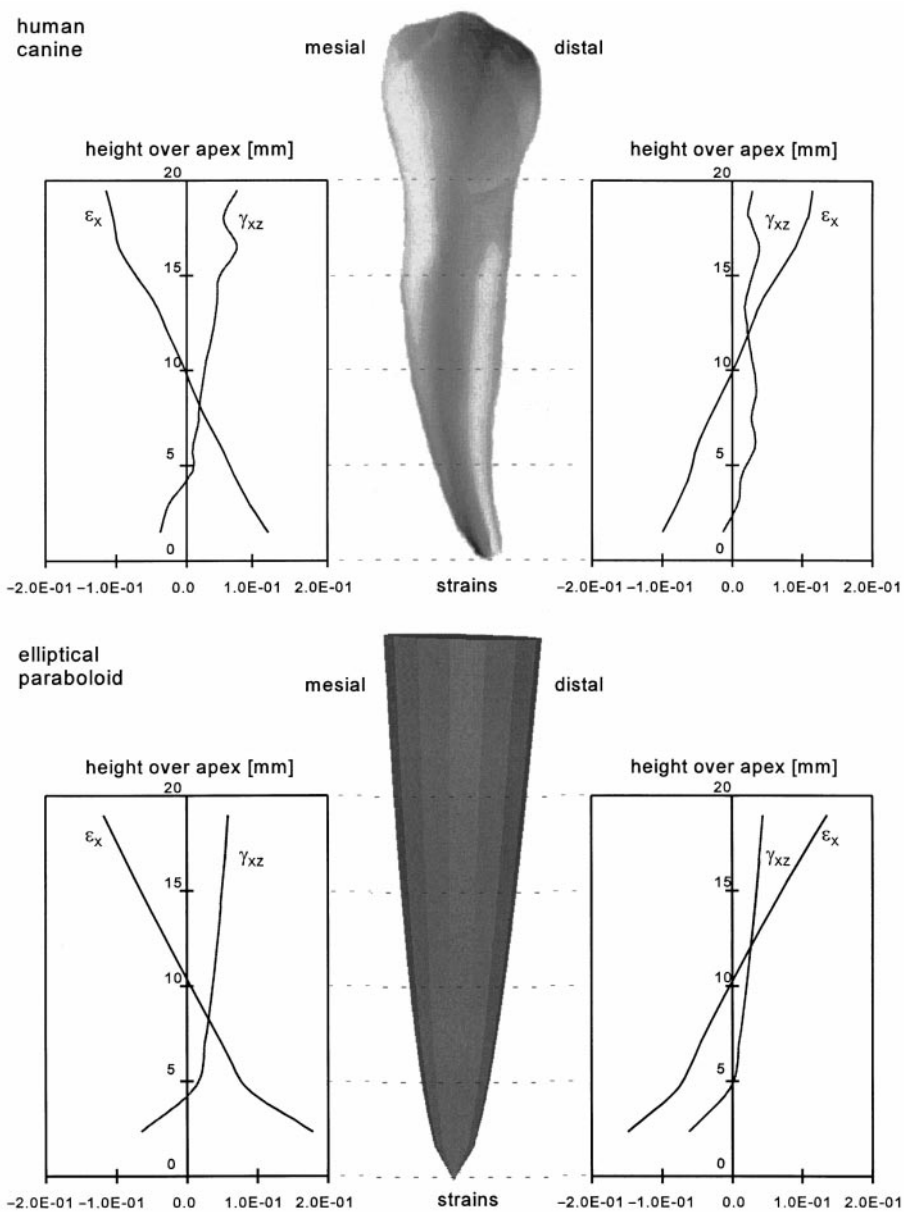

Figure 8 Strains in the mesio-distal PDL elements for a simulated uncontrolled mesial tipping. The prominent strain components are the normal strain ε_X in the distal direction and the shear strain γ_{XZ} around the *Y*-axis. For the sake of clarity all other components have been omitted.

the calculated rotational axis, i.e. the CR, lies on the long axis of the tooth for both models. Thus, the elliptical paraboloid is a good approximation to the root shape of a canine to this extent.

The location of the CR in the sagittal plane for both models however differs from values reported by other authors. Two- and three-dimensional theoretical and experimental investigations based on paraboloids and paraboloids of revolution resulted in a value of two-fifth for the planar and a value of one-third of the root length below the alveolar crest for the

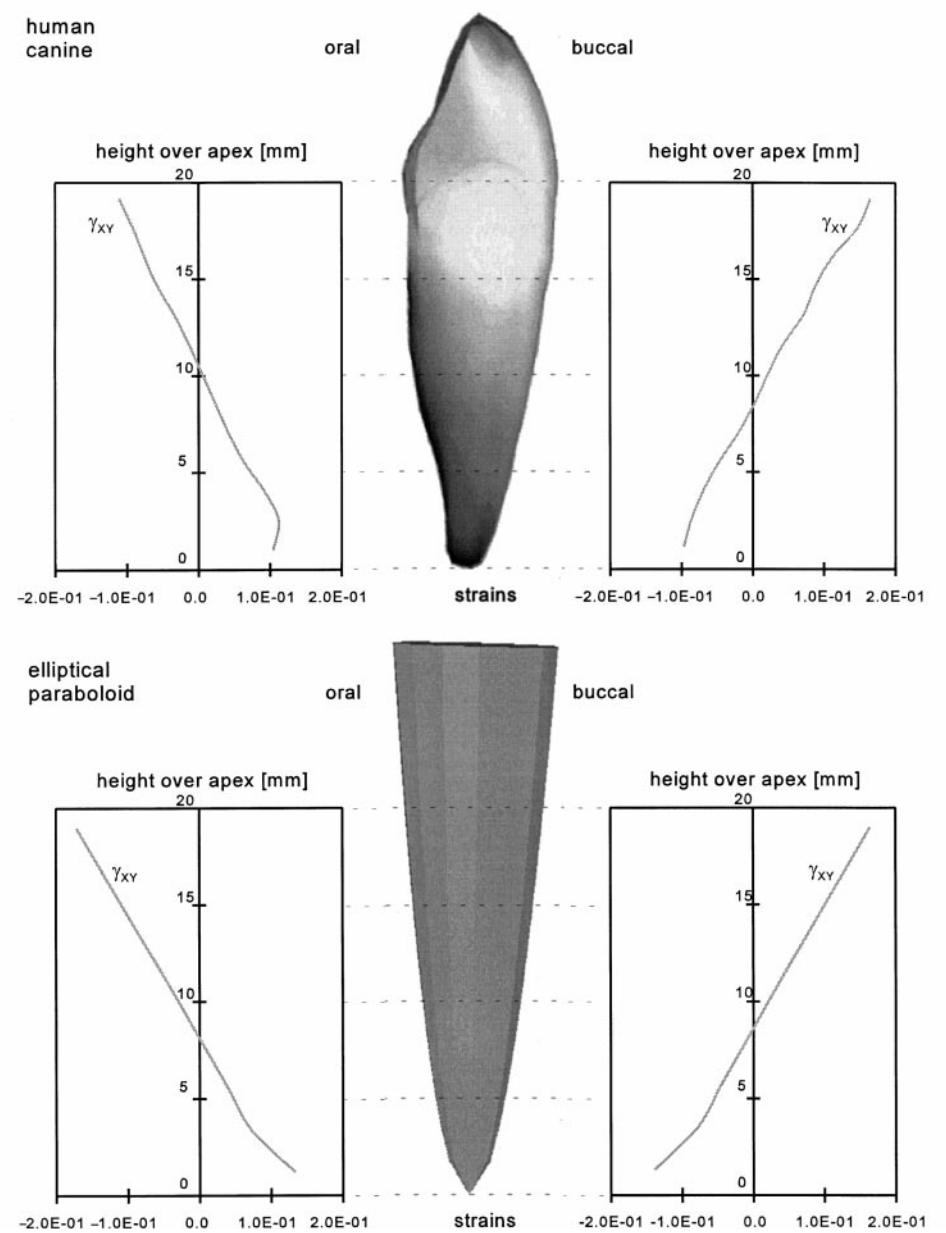

Figure 9 Strains in the oro-vestibular PDL elements. There were no normal strains in the mesio-distal direction. The prominent load mode of the PDL is a shear strain γ_{XY} around the *Z*-axis, whereas the further strain components fluctuate around a value of zero.

three-dimensional case for the location of the CR (see e.g. Burstone and Pryputniewicz, 1980). The value of one-third for the three-dimensional models was derived from the three-dimensional location of the centroid of the rotational paraboloid and verified experimentally. Calculations undertaken with an FE model of a paraboloid of revolution confirmed this value.

Analysing the current results shows that for the idealized elliptical model the CR is below one-third of the root length. For the realistic human canine model it is still further down the

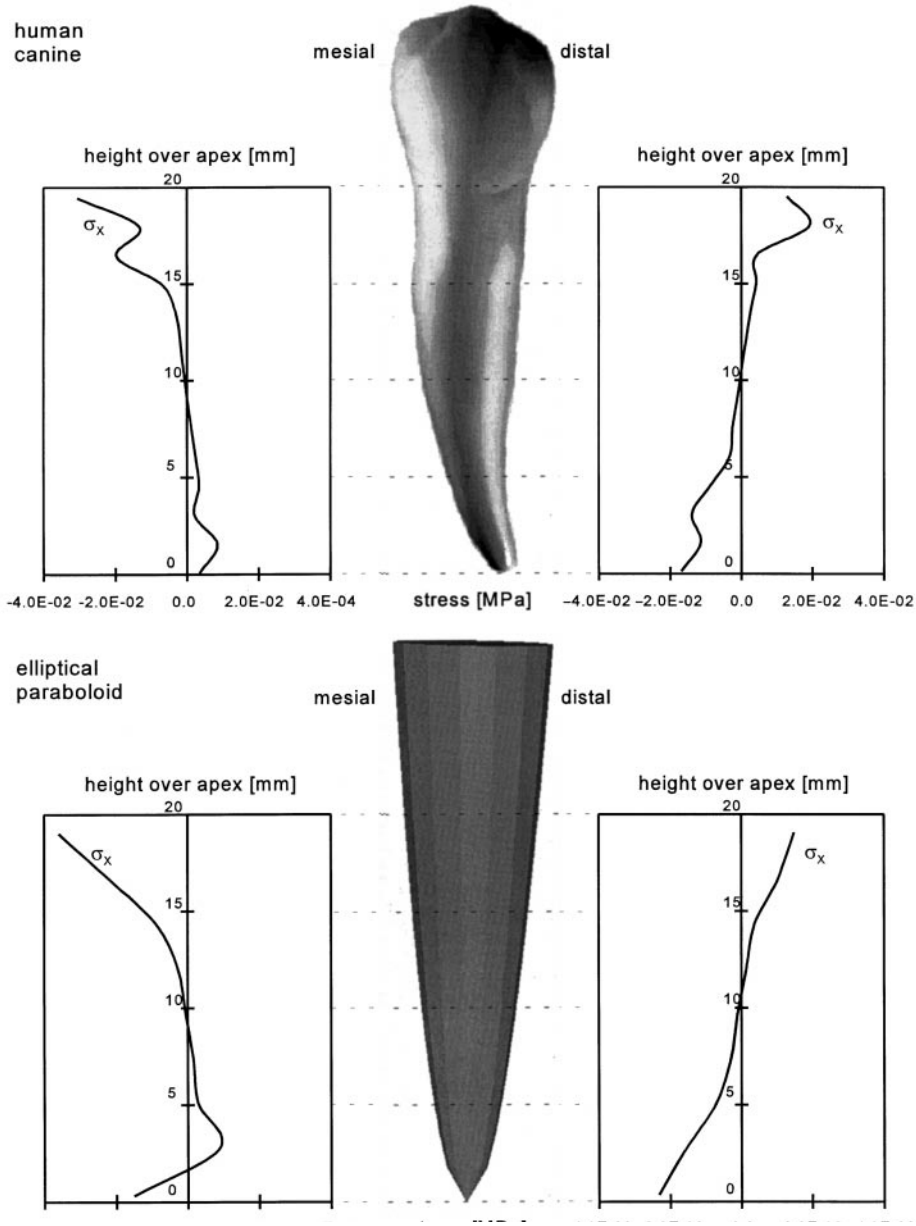

Figure 10 The most prominent stress in the PDL (mesio-distal elements), the stress component σ_x reflects the assumed non-linear behaviour of the PDL. A steep increase of stresses occurs if the ultimate strain of $\varepsilon_x = 7.5$ per cent is exceeded.

root at 8.2 mm, which is below a value of two-fifths derived from the two-dimensional studies, resulting in a location of the CR at 7.8 mm. Consequently, the round cross-section of the paraboloid of revolution seems to be an idealization that is too extreme with respect to the real geometry and results in a CR for the canine that lies too far coronally. The current results indicate that the location of the CR of a human canine is located around two-fifths of the root length and, thus, approaches the results of earlier two-dimensional studies. Thus, the elliptical

paraboloid seems to be a more appropriate approximation to the root of a canine than the paraboloid of revolution allowing the determination of the CR within an accuracy limit of approximately 10 per cent.

By knowing the CR for the idealized and for the canine model, the force systems causing uncontrolled tipping and pure translation can be determined. A detailed analysis of these movements can be achieved by calculating the ratio of the tipping performed at a given mesializing increment (R_Y/T_X). From Table 3 these ratios are $R/T = 4.55$ degrees/mm for the canine and $R/T = 4.44$ degrees/mm for the elliptical paraboloid. Thus, the tipping is only about 2 per cent higher for the human canine than for the elliptical model, which is a very good result. However, the results of the calculated bodily tooth displacement clarify the differences between an idealized and a realistic tooth geometry. The force system necessary for a pure translation of the paraboloid model can be directly deduced from the location of its CR. This was not possible for the realistic canine model. Even with an adjusted force system, it is difficult to achieve a bodily tooth movement. The reason seems to be the irregular root surface with bulges and depressions, which influences the stress/strain distribution and, thus, the tooth mobility in a decisive manner. Taking the individual variations of root geometries into account, it seems to be difficult to recommend a certain force system to achieve a bodily canine retraction, because of the individual variation of root geometries.

The type of tooth movement and the distribution of strains in the PDL is not influenced by the assumed material non-linearity of the PDL, but the stresses display a distinct non-linear distribution with root height. It seems unlikely that the orthodontic bone remodelling process is initiated by such a non-linear stress distribution. It is more likely that the strains, especially those in the PDL, can be taken as a mechanical key stimulus initiating orthodontic tooth movement. This is in accordance with the results of other studies (e.g. Middleton *et al.*, 1996) reporting high strain levels in the PDL and strains below 10^{-5} in the surrounding alveolar bone. It is important to state that all strain components, i.e. normal and shear strains, have to be considered. Neglecting the shear strains would result in a non-uniform bone remodelling process around the tooth root, which has clinically not been observed. A first numerical model to predict orthodontic bone remodelling based on FE methods was recently developed (Bourauel *et al.*, 1999). In that model, all components of the strain tensor in the ligament were used to calculate a signal for bone resorption and apposition. The results indicate that it is possible to predict clinical tooth movements based on these mechanical assumptions with a good accuracy.

Address for correspondence

Dr Christoph Bourauel
Poliklinik für Kieferorthopädie
Rheinische Friedrich-Wilhelms-Universität Bonn
Welschnonnenstr. 17
53111 Bonn
Germany

References

Abé H, Hayashi K, Sato M (eds) 1996 Data book on mechanical properties of living cells, tissues, and organs. Springer, Tokyo

Andersen K, Pedersen E, Melsen B 1991 Material parameters and stress profiles within the periodontal ligament. American Journal of Orthodontics and Dentofacial Orthopedics 99: 427–440

Arramon Y P, Cowin S C, Luo G, Sadegh A M, Zhang D 1994 Strain rate indicated as a remodeling stimulus by animal experiments. Transactions of the Orthopaedic Research Society 19: 280 (Abstract)

Atmaran G H, Mohammed H 1981 Estimation of physiologic stresses with a natural tooth considering fibrous PDL structure. Journal of Dental Research 60: 873–877

Baeten L R 1975 Canine retraction: a photoelastic study. American Journal of Orthodontics 67: 11–23

Benuzzi E, Merli M, Nesci L 1989 Ermittlung des Widerstandszentrums des Eckzahns mit Hilfe der Finite-Elemente-Analyse. Quintessenz Kieferorthopädie 3: 463–474

Bourauel C, Kobe D, Vollmer D, Drescher D 1997 Numerische Simulation kieferorthopädischer Zahnbewegung mit Hilfe der Finite-Elemente-Methode (FEM). Biomedizinische Technik 42: 339–340

Bourauel C, Freudenreich D, Vollmer D, Kobe D, Drescher D, Jäger A 1999 Simulation of orthodontic tooth movements—a comparison of numerical models. Journal of Orofacial Orthopedics 60: 136–151

Burstone C J, Pryputniewicz R J, Bowley W W 1978 Holographic measurement of tooth mobility in three dimensions. Journal of Periodontal Research 13: 283–294

Burstone C J, Pryputniewicz R J 1980 Holographic determination of centers of rotation produced by orthodontic forces. American Journal of Orthodontics 77: 396–409

Caputo A, Chaconas S J, Hayashi R K 1974 Photoelastic visualization of orthodontic forces during canine retraction. American Journal of Orthodontics 65: 250–259

Christiansen R, Burstone C J 1969 Centers of rotation within the periodontal space. American Journal of Orthodontics 55: 351–369

Cobo J, Sicilia A, Argüelles J, Suarez D, Vijande M 1993 Initial stress induced in periodontal tissue with diverse degrees of bone loss by an orthodontic force: tridimensional analysis by means of the finite element method. American Journal of Orthodontics and Dentofacial Orthopedics 104: 448–454

Davidian E J 1971 Use of a computer model to study the force distribution on the root of a maxillary central incisor. American Journal of Orthodontics 59: 581–588

Davidovitch Z, Shanfeld J L 1975 Cyclic AMP levels in alveolar bone of orthodontically treated cats. Archives of Oral Biology 20: 567–574

Davidovitch Z, Finkelson M D, Steigman S, Shanfeld J L, Montgomery P C, Korostoff E 1980 Electric currents, bone remodeling and orthodontic tooth movement. II. Increase in rate of tooth movement and periodontal cyclic nucleotide levels by combined force and electric current. American Journal of Orthodontics 77: 33–47

Dermaut L R, Kleuthgen J P, De Clerck H J 1986 Experimental determination of the center of resistance of the upper first molar in a macerated, dry human skull submitted to horizontal headgear traction. American Journal of Orthodontics and Dentofacial Orthopedics 90: 29–36

Fisher J L, Godfrey K, Stephens R I 1976 Experimental strain analysis of infant, adolescent and adult miniature swine skulls subjected to simulated mastication forces. Journal of Biomechanics 9: 333–338

Gabel A B 1956 A mathematical analysis of the function of the fibres of the periodontal membrane. Journal of Periodontology 27: 191–198

Gianelly A A 1969 Force-induced changes in the vascularity of the periodontal ligament. American Journal of Orthodontics 55: 5–11

Haase A 1996 Numerische Untersuchungen zur initialen Zahnbeweglichkeit mit Hilfe der Finite-Elemente-Methode. Thesis, Physikalisches Institut, Universität Bonn

Hay G E 1939 The equilibrium of a thin compressible membrane with application to the periodontal membrane. Canadian Journal of Research 17: 123–140

Hinterkausen M, Bourauel C, Siebers G, Haase A, Drescher D, Nellen B 1998 *In vitro* analysis of the initial tooth mobility in a novel optomechanical set-up. Medical Engineering and Physics 20: 40–49

McGuinness N J P, Wilson A N, Jones M L, Middleton J 1991 A stress analysis of the periodontal ligament under various orthodontic loadings. European Journal of Orthodontics 13: 231–242

Middleton J, Jones M, Wilson A 1996 The role of the periodontal ligament in bone modeling: the initial development of a time dependent finite elment model. American Journal of Orthodontics and Dentofacial Orthopedics 109: 155–162

Mühlemann H R 1960 10 years of tooth-mobility measurements. Journal of Periodontology 31: 110–122

Nägerl H, Burstone C J, Becker B, Kubein-Meesenburg D 1991 Centers of rotation with transverse forces: an experimental study. American Journal of Orthodontics and Dentofacial Orthopedics 109: 337–345

Nikolai R J 1974 Periodontal ligament reaction and displacement of maxillary central incisor subjected to transverse crown loading. Journal of Biomechanics 7: 93–99

Nikolai R J, Schweiker J W 1972 Investigation of root-periodontium interface stresses and displacements for orthodontic application. Experimental Mechanics 12: 406–413

Norton L A, Hanley K J, Turkewicz J 1984 Bioelectric pertubation of bone: research directions and clinical applications. Angle Orthodontist 54: 73–87

Pedersen E, Andersen K, Gjessing P E 1990 Electronic determination of centres of rotation produced by orthodontic force systems. European Journal of Orthodontics 12: 272–280

Pedersen E, Andersen K, Melsen B 1991 Tooth displacement analysed on human autopsy material by means of a strain gauge technique. European Journal of Orthodontics 13: 65–74

Pryputniewicz R J, Burstone C J, Bowley W W 1978 Determination of arbitrary tooth displacements. Journal of Dental Research 57: 663–678

Reitan K, Vanarsdall R L 1994 Biomechanical principles and reactions. In: Graber T M, Swain B F (eds) Orthodontics, current principles and techniques. C V Mosby, St Louis: pp. 96–192

Siegele D, Soltész U, Topkaya A 1986 Numerische Untersuchungen zum Rückstell- und Schwingungsverhalten von Zähnen am Beispiel eines oberen Schneidezahns. Deutsche Zahnärztliche Zeitung 41: 628–634

Steyn C L, Verwoerd W S, van der Merwe E J, Fourie O L 1978 Calculation of the position of the axis of rotation when single rooted teeth are orthodontically tipped. British Journal of Orthodontics 5: 153–156

Storey E 1973 The nature of tooth movement. American Journal of Orthodontics 63: 292–314

Sutcliff W J, Atherton J D 1980 The mechanics of tooth mobility. British Journal of Orthodontics 7: 171–178

Synge J L 1933 The tightness of the teeth, considered as a problem concerning the equilibrium of a thin incrompressible elastic membrane. Philosophical Transactions of the Royal Society of London, pp. 435–477

Takahashi N, Kitagami T, Komori T 1980 Behaviour of teeth under various loading conditions with finite element method. Journal of Oral Rehabilitation 7: 453–461

Tanne K, Sakuda M, Burstone C J 1987 Three-dimensional finite element analysis for stress in the periodontal tissue by orthodontic forces. American Journal of Orthodontics and Dentofacial Orthopedics 92: 499–505

Tanne K, Koenig H A, Burstone C J 1988 Moment to force ratios and the center of rotation. American Journal of Orthodontics and Dentofacial Orthopedics 94: 426–431

Tanne K, Nagataki T, Inoue Y, Sakuda M, Burstone C J 1991 Patterns of initial tooth displacements associated with various root lengths and alveolar bone heights. American Journal of Orthodontics and Dentofacial Orthopedics 100: 66–71

Thresher R W, Saito G E 1973 The stress analysis of human teeth. Journal of Biomechanics 6: 443–449

Turner C H, Anne V, Pidaparti M V 1997 A uniform strain criterion for trabecular bone adaption: do continuum level strain gradients drive adaption? Journal of Biomechanics 30: 549–554

Vollmer D, Bourauel C, Jäger A, Drescher D 1998 The location of the centre of resistance—a finite element analysis. European Journal of Orthodontics 20: 647 (Abstract)

Williams K R, Edmundson J T 1984 Orthodontic tooth movement analysed by the finite element method. Biomaterials 5: 347–351

Williams K R, Edmundson J T, Morgan G, Jones M L, Richmond S 1986 Orthodontic movement of a canine into an adjoining extraction site. Journal of Biomedical Engineering 8: 115–120